

# Power Electronics Design of a Solar Powered In-car Wireless Tag for Asset Tracking and Parking Applications

D Zhu<sup>1a</sup>, J Henaut<sup>b</sup> and S P Beeby<sup>a</sup>

<sup>a</sup>Electronics and Computer Science, University of Southampton, SO171BJ, UK

<sup>b</sup>STERELA, France

E-mail: dz@ecs.soton.ac.uk

**Abstract.** This paper reports the design and testing of a power conditioning circuit for a solar powered in-car wireless tag for asset tracking and parking application. Existing long range asset tracking is based on the GSM/GPRS network, which requires expensive subscriptions. The EU FP7 project CEWITT aims at developing a credit card sized autonomous wireless tag with GNSS geo-positioning capabilities to ensure the integrity and cost effectiveness for parking applications. It was found in previous research that solar cells are the most suitable energy sources for this application. This study focused on the power electronics design for the wireless tag. A suitable solar cell was chosen for its high power density. Charging circuit, hysteresis control circuit and LDO were designed and integrated to meet the system requirement. Test results showed that charging efficiency of 80 % had been achieved.

## 1. Introduction

Existing long range asset tracking systems transmit the position of the items being monitored between servers and end-users using GSM/GPRS network. Costs to use such communication channels are relatively high, which limits the applications of existing long range asset tracking systems. If the long range communication cost can be decreased, many more ‘tracking’ applications could be realised and benefit our daily life. The EU FP7 project CEWITT [1] aims at developing a credit card sized autonomous wireless tag with GNSS geo-positioning capabilities to ensure the integrity and cost effectiveness for parking applications. For this particular project, the Galileo system developed by the European Union and European Space Agency is used.

It was found in previous research that solar cells are the most suitable energy sources to power the CEWITT system [2]. This study focused on the power electronics design for the solar cell to power the wireless tag. The average power consumption of the system is around 200 mW with an operation voltage of 3 V. This means the average current consumption is 66 mA and peak current consumption can reach 100 mA. In addition, the satellite navigation chip used in this project is sensitive to ripple on its supply voltage. A maximum ripple of 30 mV is allowed. In this paper, system description is first introduced followed by the complete system design. Test results will then be presented.

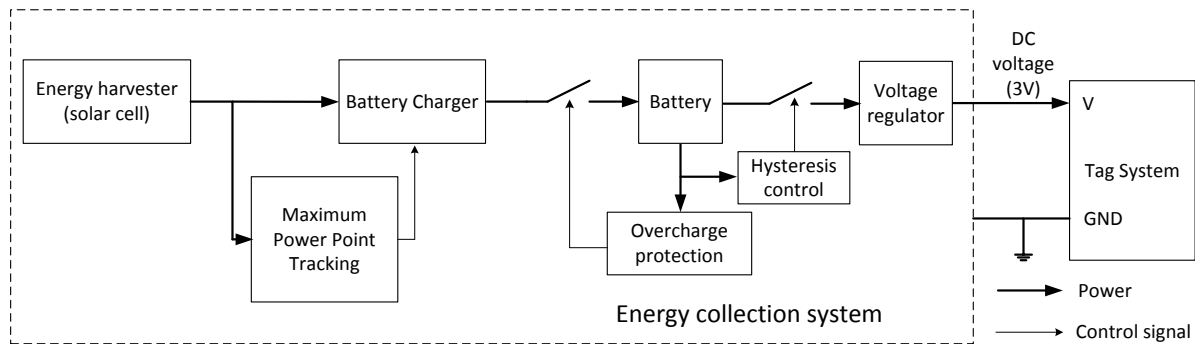
## 2. System description

Figure 1 shows the system block diagram. Maximum output power of the solar cell is extracted by using the maximum power point tracking (MPPT) technique. A solar cell charges the battery through a

---

<sup>1</sup> To whom any correspondence should be addressed.

battery charger that can prevent the battery from overcharge. The battery voltage is regulated by a low dropout regulator (LDO) to a required 3 V<sub>DC</sub>. A hysteresis control circuit cuts off the load from the battery when its voltage is below the low-end threshold and restart the system at a high-end threshold to ensure the stability of the system.



**Figure 1.** Block diagram of the energy collection system.

### 3. System design

#### 3.1. Solar cell

A comprehensive market review has been done to look for the suitable solar cell for the CEWITT tag. Considering the size restriction and the power requirement of the CEWITT tag, Ixolar SLMD121H10 was chosen as for its relatively high power density.

#### 3.2. Charging circuit

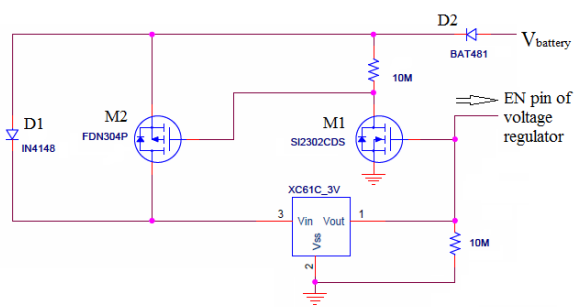
The high efficiency step-up DC/DC converter, LTC 3105, was chosen for maximum power point tracking. It can operate from input voltages as low as 225 mV and is integrated maximum power point controller (MPPC). A user programmable MPPC set point maximizes the energy that can be extracted from any power source.

The Li-Ion/Polymer shunt battery charger LTC 4071 was chosen as the battery charger. It allows simple charging of Li-Ion/Polymer batteries from very low current, intermittent or continuous charging sources and has a very low operating current of only 550 nA.

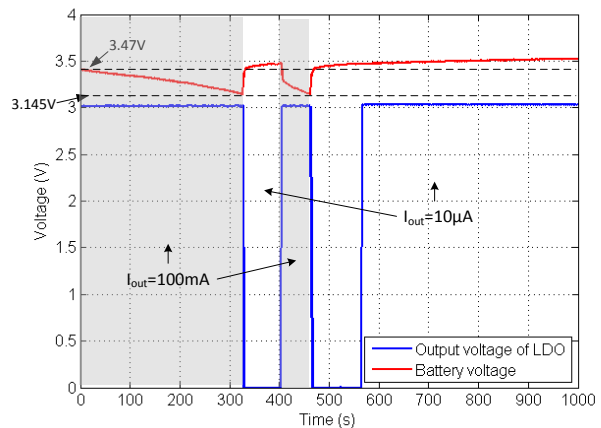
#### 3.3. Hysteresis control circuit

A hysteresis control circuit is necessary to prevent the battery from over-discharging by disconnecting the load from the battery when its voltage is below the low-end threshold,  $V_L$ , and restart the system at a high-end threshold,  $V_H$ . Two designs have been made to realise this function.

**3.3.1. Design 1.** Figure 2(a) shows the Design 1 of the hysteresis control circuit. For Design 1,  $V_H$  is 3 V plus the voltage drops on the two diodes, D1 and D2.  $V_L$  is 3 V plus the voltage drop on D2 only. When the battery voltage is above  $V_H$ , the output of the voltage detector XC61C\_3V is high, which enables the LDO and it has a 3 V DC output. The high level of the output of the voltage detector turns on the switch M1. This causes the gate of M2 to be low and the switch M2 is turned on. When M2 is on, D1 is shorted so that the output of the voltage detector will maintain the high level until the battery voltage drops below  $V_L$  when the output of the voltage detector becomes low and the LDO is disabled. In this case, M1 is off and so is M2 because its  $V_{GS}$  is 0. The LDO will remain disabled until the battery voltage exceeds  $V_H$  and the loop repeats. The advantage of this circuit is that its energy consumption is very low irrespective of the LDO being enabled or disabled. However, the two threshold voltages rely on the voltage drops of relevant diodes, which could be affected by the V/I relationship of individual diodes and the ambient temperature.



(a) circuit

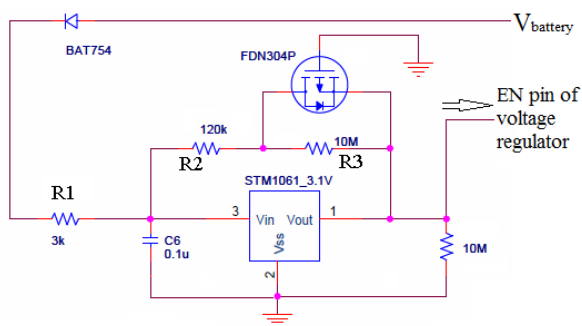


(b) test result

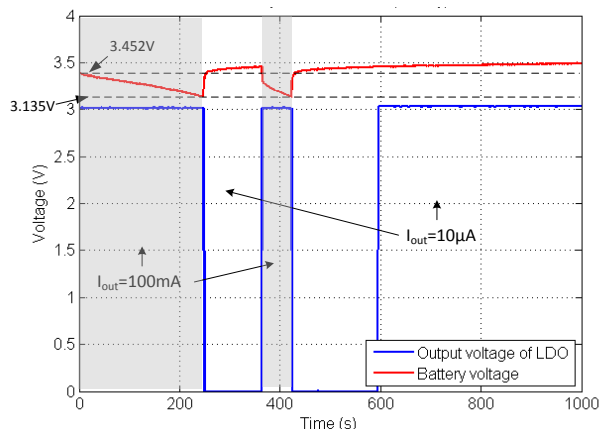
**Figure 2.** Hysteresis design 1

The test results of Design 1 are shown in Figure 2(b). The entire circuit was connected to a  $30\ \Omega$  resistive load at the beginning of the test so that the output current of the LDO is 100 mA. The battery voltage dropped gradually as the load drew energy from it. The LDO was disconnected when the battery voltage dropped to 3.145 V ( $V_L$ ). As the load is disconnected, the battery voltage recovered gradually towards its nominal voltage i.e. 3.7 V. When the battery voltage rose to 3.47 V ( $V_H$ ), the LDO was enabled and the load started to draw energy from the battery again until the battery voltage dropped to  $V_L$ . The load resistance was then adjusted to 300 k $\Omega$ , which made the output current of the LDO to be 10  $\mu$ A. With such low current consumption, the battery was able to rise beyond  $V_H$  even with the LDO enabled, due to its self-recovery and being charged by the external source. This design consumes less than 1  $\mu$ A of current.

**3.3.2. Design 2.** Figure 3(a) shows the Design 2 of the hysteresis control circuit. This design is based on the hysteresis range enlargement capability of the voltage detector with N-channel output. For Design 2,  $V_L$  is 3 V plus the voltage drop on D3 and  $V_H$  is decided by the ratio of R1 and R2. A switch M1 is used to short R3 when the LDO is in operation to provide the accurate  $V_H$  and allow R3 to be connected in series with R2 in order to reduce the current consumption when the LDO is disabled. This design can provide more accurate threshold voltages but it consumes about 25  $\mu$ A of current when the LDO is enabled. The test results of Design 2 are shown in Figure 3(b). It has similar performance as Design 1 but its threshold voltage is slightly different ( $V_L = 3.135$  V and  $V_H = 3.452$  V).



(a) circuit



(b) test result

**Figure 3.** Hysteresis design 2

### 3.4. Low DropOut regulator (LDO)

Five LDO's have been selected after a comprehensive market survey. Their specifications from datasheets are listed in Table 1. TI TPS78001 was chosen because its low dropout voltage and low current consumption. TI TPS71730, TI TPS79930 and TI LP5900 were chosen because of their high ripple rejection. However, their current consumption is very high. The Torex XC6215 has been used in other satellite navigation systems and it was used in the test as a reference. It was found that LP5900 has the lowest ripple and TPS78001 has the lowest dropout voltage when their output current is 100 mA. Considering that the power consumption of LP5900 is considerably higher than TPS78001, TPS78001 was chosen as the LDO for this application.

**Table 1.** Comparison of various LDOs.

|                 | $I_L=10\mu A$ |                      | $I_L=100mA$ |                      |                      |                   |
|-----------------|---------------|----------------------|-------------|----------------------|----------------------|-------------------|
|                 | Ripple (mV)   | $V_{out}$ of LDO (V) | Ripple (mV) | $V_{out}$ of LDO (V) | Dropout Voltage (mV) | $I_q$ ( $\mu A$ ) |
| <b>TPS78001</b> | 14.2          | 3.015                | 16.5        | 3.0106               | -4.4                 | 4                 |
| <b>TPS71730</b> | 1.5           | 3.0101               | 1.9         | 2.9819               | -28.2                | 100               |
| <b>TPS79930</b> | 1.3           | 3.0370               | 65.3        | 3.0671               | +30.1                | 40                |
| <b>LP5900</b>   | 1.1           | 3.0025               | 0.799       | 2.9943               | -8.2                 | 140               |
| <b>XC6215</b>   | 2.2           | 2.9991               | 7.3         | 2.9702               | -28.9                | N/A               |

### 4. Test results

Figure 4 shows the final circuit design. Hysteresis design 1 was chosen as it consumes less energy. The battery used in the test was a 300mAh LiPo battery. The charging circuit was tested in a sunny spell day and a cloudy day.

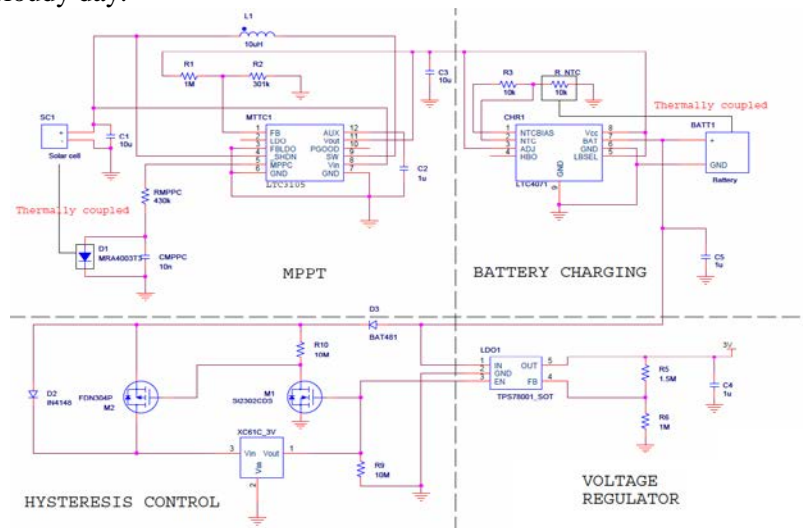


**Figure 4.** Final circuit design.

#### 4.1. Sunny day

This test was carried out in a sunny spell day when the illumination was between 15 and 30 klux. Figure 5(a) shows the voltage of the solar cell and the battery and Figure 5(b) shows the input and charging power. During the test, the battery was discharged at 100 mA twice. For the first discharge, the duration was 1 min 35 sec and the battery voltage dropped from 3.287 V to 2.989 V. The battery voltage was recovered to 3.287 V after being charged for 16 min 6 sec. The average charging power during this period was 27.8 mW. For the second discharge, the duration was 5 min 5 sec. The battery voltage dropped from 3.373 V to 2.898 V. The battery voltage was recovered to 3.373 V after being charged for 47 min 51 sec. The average charging power during this period was 27.5 mW. Average charging efficiency was 80 %.

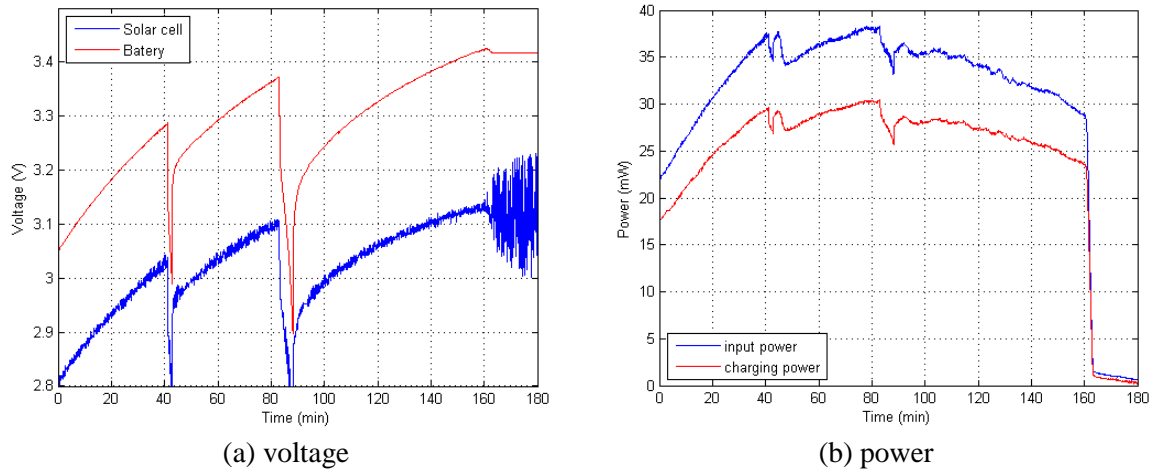


**Figure 5.** Test results in a sunny day.

#### 4.2. Cloudy day

This test was carried out in a cloudy day with a period of sunny spell lasting 20 minutes. The illumination was below 15 klux for most of the time. Figure 6(a) shows the voltage of the solar cell and the battery and Figure 6(b) shows the input and charging power. The average charging power in this case was 9.1 mW. Average charging efficiency was 75 %.

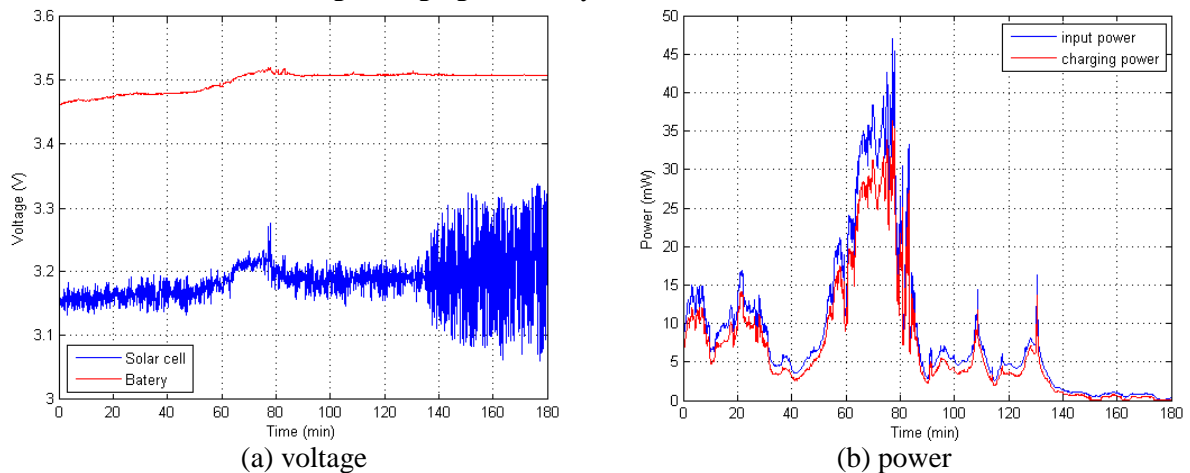


**Figure 6.** Test results in a cloudy day.

### 5. Conclusions

This paper presents the design of a power conditioning circuit for a solar powered wireless tag. Ixolar SLMD121H10 was chosen as the solar cell for its suitable size and high power density. MPPT and charging circuit ICs were chosen to achieve maximum charging efficiency of 80 %. Hysteresis circuit was designed to protect the battery from over discharging. A suitable LDO was selected to minimise ripple of its output to meet the requirement of the satellite navigation IC.

### 6. References

- [1] EU FP7 project CEWITT, <http://www.cewitt.ecs.soton.ac.uk/>
- [2] Zhu D, Wang L, Henaut J and Beeby S 2014 *Proc. Euroensors 2014*.

### Acknowledgments

This work is supported by the European Union Seventh Framework Programme (FP7) research project CEWITT (<http://www.cewitt.ecs.soton.ac.uk/>).